

MOL #93229

Clemizole hydrochloride is a novel and potent inhibitor of transient receptor potential channel  
TRPC5

Julia M. Richter, Michael Schaefer and Kerstin Hill

Rudolf-Boehm-Institute of Pharmacology and Toxicology,  
University of Leipzig, 04107 Leipzig, Germany

Running title page:

**Running title:** Clemizole inhibit TRPC5 channel activity

**Corresponding author:** Kerstin Hill, Institute of Pharmacology and Toxicology, Härtelstr. 16-

18, 04107 Leipzig; Germany, phone: +49-341-9724616, fax: +49-341-9724609; e-mail:

[kerstin.hill@medizin.uni-leipzig.de](mailto:kerstin.hill@medizin.uni-leipzig.de)

**Document statistics:**

Number of text pages: 26 (Abstract, Introduction, M & M, Results and Discussion: 13)

Number of figures: 5

Number of supplementary figures: 2

Number of references: 38

Number of words in the Abstract: 245

Number of words in Introduction: 574

Number of words in Discussion: 627

**Abbreviations:**  $[Ca^{2+}]_i$ , intracellular free  $Ca^{2+}$  concentration; AITC, allylthiocyanate; 2-APB, 2-Aminoethoxydiphenyl borate; CFP, cyan fluorescent protein; DAG, diacylglycerol; GPCR, G-protein coupled receptor; HBS, HEPES-buffered solution;  $IC_{50}$ , half maximal inhibitory concentration;  $InsP_3$ , Inositol 1,4,5-trisphosphate receptor; LOPAC, Library of pharmacologically active compounds;  $M3R\Delta i3$ , muscarinic M3 receptor with a deletion in the third intracellular loop;  $PIP_2$ , phosphatidylinositol 4,5-bisphosphate; PKC $\epsilon$ , protein kinase C $\epsilon$ ; PLC, phospholipase C; PregS, pregnenolone sulphate; tet, tetracycline; T-Rex, tetracycline-regulated expression; TRPC5, transient receptor potential channel C 5; YFP, yellow fluorescent protein;

## Abstract

TRPC5 is a nonselective,  $\text{Ca}^{2+}$  permeable cation channel which belongs to the large family of transient receptor potential channels. It is predominantly found in the central nervous system with a high expression density in the hippocampus, the amygdala and the frontal cortex. Several studies confirm that TRPC5 channels are implicated in the regulation of neurite length and growth cone morphology. We identified clemizole as a novel inhibitor of TRPC5 channels. Clemizole efficiently blocks TRPC5 currents and  $\text{Ca}^{2+}$  entry in the low micromolar range ( $\text{IC}_{50} = 1.0 - 1.3 \mu\text{M}$ ), as determined by fluorometric  $[\text{Ca}^{2+}]_i$  measurements and patch clamp recordings. Clemizole blocks TRPC5 currents irrespectively of the mode of activation, e.g. stimulation of GPCR, hypoosmotic buffer conditions or by the direct activator riluzole. Electrophysiological whole cell recordings revealed that the block was mostly reversible. Moreover, clemizole was still effective in blocking TRPC5 single channels in excised inside-out membrane patches, hinting to a direct block of TRPC5 by clemizole. Based on fluorometric  $[\text{Ca}^{2+}]_i$  measurements, clemizole exhibits a 6-fold selectivity for TRPC5 over TRPC4 $\beta$  ( $\text{IC}_{50} = 6.4 \mu\text{M}$ ), the closest structural relative of TRPC5 and an almost 10-fold selectivity over TRPC3 ( $\text{IC}_{50} = 9.1 \mu\text{M}$ ) and TRPC6 ( $\text{IC}_{50} = 11.3 \mu\text{M}$ ). TRPM3 and M8 as well as TRPV1, V2, V3 and V4 channels were only weakly affected by markedly higher clemizole concentrations. Clemizole was not only effective in blocking heterologously expressed TRPC5 homomers but also TRPC1:TRPC5 heteromers as well as native TRPC5-like currents in the U-87 glioblastoma cell line.

## Introduction

All TRP channels have in common that four subunits assemble to form the cation-permeable pore. Within the group of TRPC channels, TRPC5 subunits can arrange as homomeric or heteromeric channel complexes together with TRPC1 or TRPC4 (Hofmann *et al.*, 2002). Heterologous expression studies revealed that heterotetramers composed of TRPC1 and TRPC5 subunits exhibit altered biophysical properties regarding the current-voltage relation and single channel conductance compared to the TRPC5 homotetramers (Strubing *et al.*, 2001). TRPC1 and TRPC5 channel proteins display an overlapping expression pattern in the mammalian brain. Both are highly expressed in parts of the limbic system like hippocampus and amygdala and in the frontal cortex (Strubing *et al.*, 2001; Fowler *et al.*, 2007). Up to now, the physiological function of TRPC5 in the brain has not entirely been understood. The channel is involved in the regulation of neurite length and growth cone morphology and the motility of hippocampal neurons (Greka *et al.*, 2003; Hui *et al.*, 2006). Studies on TRPC5 knockout mice revealed that granule neurons of the hippocampus and cerebellar cortex exhibit longer and more highly branched dendrites with an impaired dendritic claw differentiation. The impaired dendrite patterning in the cerebellar cortex correlates with deficits in gait and motor coordination observed in these animals (Puram *et al.*, 2011). Moreover, TRPC5-deficient mice appeared to have a diminished fear-related behaviour when confronted with innate aversive stimuli (Riccio *et al.*, 2009). Recent studies further revealed a role of TRPC5 in podocytes, demonstrating that the pathogenic remodelling in proteinuria mouse models can be attributed to the activation of TRPC5 channels. Accordingly, TRPC5-deficient mice were less sensitive to LPS-induced albuminuria (Greka and Mundel, 2011; Schaldecker *et al.*, 2013), making a pharmacological inhibition of TRPC5 a promising target to protect from the destruction of the glomerular filter barrier in kidney injury.

Several inhibitors of TRPC5 activity have been published, such as SKF96356 and flufenamic acid. These compounds are poorly selective modulators known to affect multiple TRP channels from different subfamilies, voltage-gated channels, intracellular  $\text{Ca}^{2+}$  release channels and chloride channels (Merritt *et al.*, 1990; Hofmann *et al.*, 1999; Inoue *et al.*, 2001; Gardam *et al.*, 2008). 2-Aminoethoxydiphenyl borate (2-APB), an inhibitor of the inositol 1, 4, 5-trisphosphate receptor ( $\text{IP}_3\text{R}$ ), blocks TRPC5 currents reversibly and in a voltage-dependent manner (Xu *et al.*, 2005). However, 2-APB is neither a potent ( $\text{IC}_{50} = 20 \mu\text{M}$ ) nor a specific TRPC5 blocker since it affects other TRPC, TRPV, TRPM and TRPP channels (Hu *et al.*, 2004; Lievremont *et al.*, 2005; Xu *et al.*, 2005; Li *et al.*, 2006; Kovacs *et al.*, 2012).

Recently a novel potent TRPC4 blocker was identified (Miller *et al.*, 2011). ML204 inhibits TRPC4 and C5 currents, induced by  $\mu$ -opioid or muscarinic receptor stimulation. The blocker has a higher selectivity for TRPC4 than for TRPC5, inhibiting just 65 % of TRPC5 channel activity at a concentration of  $10 \mu\text{M}$  ( $\text{IC}_{50} = 9.2 \mu\text{M}$ , (Miller *et al.*, 2010)). Furthermore, ML204 exhibits also moderate inhibitory effects on muscarinic receptors.

In the present study we identified clemizole hydrochloride as a novel blocker of the transient receptor potential (TRP) channel TRPC5 with a half maximal inhibitory concentration of  $1.1 \mu\text{M}$ . Clemizole inhibits TRPC5 independent from cytosolic components or phospholipase C activity, suggesting a rather direct action of the drug on the channel. Clemizole was efficient to block heterologously expressed homomeric TRPC5 channels as well as heteromeric TRPC1:TRPC5 channels. Also natively expressed riluzole-evoked TRPC5 currents in the U-87 glioblastoma cell line could be inhibited by clemizole.

## Materials and Methods

### *Cell culture and reagents*

A T-REx-HEK293 cell line (Invitrogen, Corp., Carlsbad, CA, USA) was used and stably transfected with murine TRPC5 (T-REx<sub>TRPC5</sub>) in order to generate an inducible tetracycline-regulated expression system of TRPC5. Cells were treated with 1 µg/ml tetracycline (Tet+, Sigma-Aldrich, St. Louis, MO, USA) for 48 h before measurements to induce TRPC5 expression. For control experiments, parental T-REx-HEK293 cells were used. Cells were grown in Dulbecco's modified Eagle's medium (DMEM, PAA Laboratories, Pasching, Austria), containing 10% fetal calf serum, 2 mM L-glutamine, 100 units/ml penicillin, 0.1 mg/ml streptomycin, 100 µg/ml zeocin. Culture medium for T-REx<sub>TRPC5</sub> cells was additionally supplemented with 15 µg/ml blasticidin (Invitrogen). Other TRP channels, stably expressed in HEK293 (YFP-tagged human TRPC3, YFP-tagged human TRPC6, YFP-tagged mouse TRPC7, CFP-tagged rat TRPV1, YFP-tagged rat TRPV2, YFP-tagged rat TRPV3, YFP-tagged mouse TRPV4, CFP-tagged human TRPM8, human TRPA1) were generated and maintained as described previously (Hill and Schaefer, 2007; Urban *et al.*, 2012). The generation of the stable myc-tagged rat HEK<sub>TRPM3</sub> cell line was described elsewhere (Fruhwald *et al.*, 2012).

### *Cell transfection*

HEK293 cells were transiently transfected using jetPei transfection reagent according to the manufacturer's instructions (Peqlab, Erlangen, Germany). For some experiments, we transiently co-transfected YFP-tagged mouse TRPC4β (in a pcDNA3 vector) and rat M3RΔi3 (in pcDNA5/FRT) or pcDNA3 plasmids encoding YFP-tagged mouse TRPC5 or YFP-tagged human TRPC1. The plasmid concentrations of TRPC1:TRPC5 and TRPC4β-M3RΔi3 were

used in equal amounts. Cells were grown in Earle's Minimum Essential Medium (MEM, PAA Laboratories) supplemented with 10% fetal calf serum, 2 mM L-glutamine, 100 units/ml penicillin, 0.1 mg/ml streptomycin. The transfection was conducted at a cell confluency of 80%.

#### *Confocal laser scanning microscopy*

The subcellular distribution of YFP-tagged protein kinase C $\epsilon$  (PKC $\epsilon$ ) was visualized by using an inverted confocal laser scanning microscope (LSM510-META, 100 $\times$ /1.46 Plan Apochromat, Carl Zeiss, Oberkochen, Germany). The cells were seeded on coated (25  $\mu$ g/ml poly-L-lysine (Sarstedt, Nümbrecht, Germany)) 25 mm glass coverslips. The fluorescence was excited at 488 nm wavelength. The emitted light was filtered through a 505-550 nm bandpass filter.

#### *Intracellular Ca<sup>2+</sup> analysis*

For the primary compound screen and to generate concentrations response curves, cells were loaded with fluo-4/AM (4  $\mu$ M, 30 min, 37°C; Invitrogen) dissolved in HEPES-buffered solution (HBS) containing (in mM): 134 NaCl, 6 KCl, 1 MgCl<sub>2</sub>, 1 CaCl<sub>2</sub>, 10 HEPES, pH 7.4 adjusted with NaOH. Fluorometric assays were performed in a 384-well microtitre plate format (15,000 cells/well, Corning, USA). All cells were measured in suspension except of T-REX<sub>TRPC5</sub> cells, which were seeded into the microtitre plate and treated with 1  $\mu$ g/ml tetracycline 48 h before measurement to induce channel expression. A custom-made fluorescence plate imaging device was used to record changes in fluorescence expressed as  $\Delta F/F_0$  (Norenberg *et al.*, 2012). In some experiments, agonists of endogenously expressed GPCR of HEK293 cells were used. These measurements required a pre-treatment with thapsigargin (2  $\mu$ M, 5 min) to deplete InsP<sub>3</sub>-sensitive Ca<sup>2+</sup> stores. For the primary screening

assay, compounds of the Spectrum Collection (MicroSource, Gaylordsville, CT, USA), or of a LOPAC<sup>1280</sup> (Sigma-Aldrich) compound collection were added to T-REX<sub>TRPC5</sub> cells at a final concentration of 20  $\mu$ M. Afterwards, a mixture of agonists (Amix: 300  $\mu$ M ATP, 300  $\mu$ M carbachol and 0.5 U/ml thrombin) was applied to induce TRPC5 activity via GPCR signalling. For single-cell  $[Ca^{2+}]_i$  analysis, cells were seeded onto poly-L-lysine-coated glass coverslips and allowed to attach for 24 h - 48 h. T-REX<sub>TRPC5</sub> cells were treated as described before. At a final confluency of about 60%, cells were loaded with 2  $\mu$ M fura-2/AM (Molecular Probes, Eugene, OR, USA) for 30 min at 37 °C in HBS buffer. The coverslips were mounted in a bath chamber of an inverted microscope (Axiovert 100, Carl Zeiss) equipped with a monochromator-assisted (TILL Photonics, Gräfelfing, Germany) digital epifluorescence videomicroscopy. The fluorescence was sequentially excited at 340, 358 and 380 nm, and the emitted light was filtered with a 512 nm long-pass filter. The measurements were recorded by a 12-bit cooled charge-coupled device camera (IMAGO; TILL Photonics, Graefelfing, Germany). The calcium concentration was calculated as described before (Lenz *et al.*, 2002).

### *Electrophysiology*

Patch clamp recordings were performed in the whole-cell configuration using a Multiclamp 700B amplifier together with a digidata 1440A digitizer (Molecular Devices, Sunnyvale, CA) under pCLAMP 10 software. Cells were seeded on glass coverslips 24 h - 48 h before measurement with 20-30 % cell confluency. The coverslips were transferred to a continuously perfused bath chamber integrated in a stage of an inverted microscope. The standard bath solution for whole cell recordings contained (in mM): 130 NaCl, 5 KCl, 1.2 MgCl<sub>2</sub>, 1.5 CaCl<sub>2</sub>, 8 D-glucose and 10 HEPES, pH 7.4 adjusted with NaOH. The standard pipette solution contained (in mM): 115 CsCl, 2 MgCl<sub>2</sub>, 5 Na<sub>2</sub>ATP, 0.1 NaGTP, 5.7 CaCl<sub>2</sub>, 10 HEPES and 10 EGTA, pH 7.2 adjusted with CsOH, yielding a calculated free calcium concentration of 200



nM (MaxChelator; (<http://maxchelator.stanford.edu>)). For some experiments, the pipette solution was supplemented with 500  $\mu$ M of GTP $\gamma$ S (Sigma-Aldrich). For inside out recordings, the pipette solution consisted of (in mM): 140 NaCl, 5 CsCl, 2 MgCl<sub>2</sub>, and 10 mM HEPES, pH 7.4 adjusted with NaOH. The bath solution contained (in mM): 140 CsCl, 4 Na<sub>2</sub>ATP, 2 MgCl<sub>2</sub>, 0.38 CaCl<sub>2</sub>, 1 EGTA, 10 HEPES, pH 7.2 adjusted with CsOH (100 nM free calcium concentration). To measure mTRPC4 $\beta$  currents, the pipette solution contained (in mM): 135 CsCl, 2 MgCl<sub>2</sub>, 0.362 CaCl<sub>2</sub>, 1 EGTA and 30 HEPES, pH 7.2 adjusted with CsOH, yielding a free calcium concentration of 100 nM. Voltage ramps from -100 to +100 mV (500 ms duration) were applied in 1-s intervals. Currents were filtered at 3 kHz (four-pole Bessel filter) and sampled at 5 kHz. Whole cell series resistances were compensated by 70%. Adherent cells were transferred into a recording chamber holding a volume of 500  $\mu$ l. Drugs were applied using a gravity-driven perfusion system.

#### *Data analysis*

Fura-2-based single cell [Ca<sup>2+</sup>]<sub>i</sub> measurements are representative for several independent recordings. Grey lines represent single cell traces, black lines display corresponding mean values. Data of fluo-4-based Ca<sup>2+</sup> measurements are depicted as mean  $\pm$  SD and were normalized to baseline (grey circles) or to the maximum Ca<sup>2+</sup> response to the channel-specific agonist (black circles). The IC<sub>50</sub> values were calculated by fitting the data to a Hill's equation using OriginPro 8 (OriginLab Corporation, Northampton, MA, USA) software. Data of electrophysiological recordings are presented as mean  $\pm$  SEM. Statistical comparison of two datasets was performed with the Student's t-test using GraphPad (GraphPad software, La Jolla, CA, USA). P < 0.05 (\*) was considered as being statistically significant.

## RESULTS

### *Clemizole inhibits TRPC5 channel activity*

In order to identify novel modulators of TRPC5, we performed a 384-well-based medium-throughput screen using the Spectrum Collection and LOPAC<sup>1280</sup> compound libraries. A stably transfected HEK293 cell line, expressing TRPC5 channels upon tetracycline treatment, was used for the screening assay. To prevent a release of intracellular Ca<sup>2+</sup> upon GPCR stimulation, T-REX<sub>TRPC5</sub> cells were pre-treated with thapsigargin (2 μM for 5 min) prior to measurement. The compound screen revealed that TRPC5 channel activity, which was induced by a mixture of GPCR-agonists (Amix: 300 μM ATP, 300 μM carbachol and 0.5 U/ml thrombin), was efficiently blocked upon clemizole application. To verify the primary screening data, we performed concentration-response measurements by using Ca<sup>2+</sup> assays in fluo-4-loaded cells (Fig. 1A, B). The concentration-response curves confirmed a concentration-dependent block of TRPC5 by clemizole (chemical structure shown in Fig. 1 C) and revealed an apparent IC<sub>50</sub> of 1.1 ± 0.04 μM (Fig. 1 A, black circles). To examine the effects on GPCR, G-protein or phospholipase C, non-transfected parental T-REx cells were stimulated with the same agonist mix and remained thapsigargin-untreated. Ca<sup>2+</sup> responses in these cells were not affected by clemizole (Fig. 1B). To test whether also other modes of TRPC5 activation could be blocked by clemizole, we performed fura-2-based single cell Ca<sup>2+</sup> imaging experiments. Clemizole (10 μM) did not only inhibit TRPC5 currents induced by Amix (Fig. 1D) but also by riluzole (Fig. 1E; 50 μM) or by hypoosmotic buffer conditions (Fig. 1F; 200 mosmol kg<sup>-1</sup>). To ensure that [Ca<sup>2+</sup>]<sub>i</sub> signals did not arise by depletion of internal Ca<sup>2+</sup> stores, cells were again pre-treated with thapsigargin (2 μM).

Additional whole cell patch clamp recordings confirmed the calcium imaging data. As reported previously (Richter *et al.*, 2014), a basal activity of TRPC5 channels in the absence of agonists was evident during the recordings. Amix-induced TRPC5 currents were

MOL #93229

completely blocked upon clemizole (10  $\mu$ M) application (Fig. 2A-C), even below the basal current level at the beginning of the recording (Fig. 2C). TRPC5 currents provoked by riluzole (50  $\mu$ M) were also blocked by 10  $\mu$ M clemizole (Fig. 2D-F). The clemizole-mediated block was mostly reversible and TRPC5 currents could repetitively be stimulated by riluzole (Fig. 2 E). The IC<sub>50</sub> value from the calcium assays for the clemizole-blocked TRPC5 channels was further validated in whole cell patch clamp experiments, yielding an IC<sub>50</sub> of  $1.05 \pm 0.3$   $\mu$ M for the outward, and  $1.34 \pm 0.4$   $\mu$ M for the inward current (Fig. 2G).

*Clemizole does not inhibit GPCR-, G-protein- or PLC signaling and soluble cytosolic components are not required for the block of TRPC5.*

We conducted whole cell patch clamp recordings on T-REX<sub>TRPC5</sub> cells and applied GTP $\gamma$ S (500  $\mu$ M) via the patch pipette (Fig. 3A-C). This non-hydrolysable analogue of guanosine triphosphate (GTP) activates G $\alpha$ q-proteins and induces TRPC5 currents (Schaefer *et al.*, 2000). The resulting TRPC5 currents could be blocked by clemizole (10  $\mu$ M), indicating that an inhibition of GPCR-signaling was not causal for the block. To determine whether clemizole affects phospholipase C (PLC) activity, we used a HEK293 cell line that stably expresses protein kinase C $\epsilon$  (HEK<sub>PKC $\epsilon$</sub> , (Schaefer *et al.*, 2001)). Upon stimulation of G $\alpha$ q protein-coupled GPCRs via Amix, PLC is activated and generates diacylglycerol (DAG) from phosphatidylinositol 4,5-bisphosphate (PIP<sub>2</sub>). DAG then induces the translocation of the PKC $\epsilon$  to the plasma membrane. We visualized this translocation by using an YFP-tagged construct of PKC $\epsilon$  (Supplementary figure 1). Untreated HEK<sub>PKC $\epsilon$ -YFP</sub> cells (control) present an evenly distributed cytosolic fluorescence. This subcellular distribution was unaltered upon clemizole (10  $\mu$ M) application. Additional application of Amix induced, as expected, a translocation of PKC $\epsilon$  to the plasma membrane, indicating that clemizole did not affect PLC activity.

We next wanted to know whether intracellular soluble molecules contribute to the block of TRPC5 channels by clemizole. To this end, we conducted electrophysiological experiments in the inside out configuration. As reported previously (Richter *et al.*, 2014), riluzole causes a strong increase in the open probability of TRPC5 channels. At -80 mV the riluzole-activated TRPC5 channels had a conductance of  $56 \pm 4$  pS ( $n = 11$ ). The addition of 20  $\mu$ M clemizole was still effective in blocking TRPC5 channels when applied to the cytosolic side of the channel, indicating a direct action of clemizole on riluzole-activated TRPC5 channels (Fig. 3D).

*Clemizole-mediated action on other transient receptor potential channels.*

To examine whether clemizole affects other TRP channels, we performed fluo-4-based  $\text{Ca}^{2+}$  assays on HEK293 cells, overexpressing various closely or more distantly related TRP channels. Cells were first treated with different concentrations of clemizole and, subsequently, the respective TRP channel-specific agonist was applied. All cell lines expressing canonical TRP channels (TRPC) were pre-treated with thapsigargin prior to measurements to deplete InsP3-sensitive intracellular  $\text{Ca}^{2+}$  stores. The channel activity of TRPC4 $\beta$  was induced by carbachol (300  $\mu$ M, Fig. 4D), and of TRPC3, C6 and C7 by Amix (Fig. 4A-C). Within the TRPC subfamily, apart from TRPC5 also TRPC3, C4, C6 and C7 were affected by clemizole. However,  $\text{IC}_{50}$  values for the block were considerably higher compared to TRPC5. TRPC4 $\beta$ , the closest structural relative of TRPC5, was blocked by clemizole with an  $\text{IC}_{50}$  of  $6.4 \pm 0.9$   $\mu$ M (Fig. 4D). Whole cell patch clamp recordings indicated that the block of TRPC4 $\beta$  by clemizole was relatively slow and not complete at a concentration of 10  $\mu$ M. 2-APB (75  $\mu$ M) further blocked TRPC4 $\beta$  currents, even below the basal current densities at the beginning of the recording (Fig. 4E-G). As the slow block by clemizole was superimposed by a rapid and in most cases complete run-down of channel activity, the calculated  $\text{IC}_{50}$  values for the

clemizole-induced block of  $4.43 \pm 0.5 \mu\text{M}$  (for the outward current) and of  $1.46 \pm 0.3 \mu\text{M}$  (for the inward current) (Fig. 4H) might not be accurate.

Analyzing TRPC3- and TRPC6-overexpressing cells by fluorometric  $\text{Ca}^{2+}$  assays revealed, that clemizole possesses an almost 10-fold selectivity for TRPC5 over TRPC3 ( $\text{IC}_{50} = 9.1 \mu\text{M}$ ) and TRPC6 ( $\text{IC}_{50} = 11.3 \mu\text{M}$ ). TRPC7 was even less sensitive to clemizole treatment ( $\text{IC}_{50} = 26.5 \mu\text{M}$ ). The more distantly related TRPM3 and M8 (melastatin related) or TRPV1, V2, V3 and V4 (vanilloid receptor-like) channels were only weakly affected by clemizole at high concentrations above  $20 \mu\text{M}$ . Clemizole also activated the pleiotropic irritant sensor TRPA1 at concentrations  $> 10 \mu\text{M}$  (Supplementary figure 2).

#### *Clemizole blocks heteromeric TRPC1:TRPC5 channels*

Heterologous co-expression studies of TRPC1 and TRPC5 have shown that these channels can assemble as heteromeric ion channels with distinct current-voltage relationships compared to currents through homomeric TRPC5 channels (Strubing *et al.*, 2001). In order to test whether clemizole can also block heteromeric TRPC1:TRPC5 channels, we co-transfected HEK293 cells with a 1:1 mixture of expression plasmids encoding TRPC1 and TRPC5 (HEK<sub>TRPC1:TRPC5</sub>). As reported previously, cells, expressing only TRPC1, were not stimulated by riluzole ( $50 \mu\text{M}$ ) and possess only low basal current densities of about  $10 \text{ pA/pF}$  at  $+100 \text{ mV}$  (Richter *et al.*, 2014). A co-transfection of TRPC1 and TRPC5 resulted in an elevation of the basal current densities (Fig. 5A-C), and challenging the cells with riluzole ( $50 \mu\text{M}$ ) induced a strong outwardly rectifying current, typical to heteromeric TRPC1:TRPC5 currents (Strubing *et al.*, 2001), which could be blocked by clemizole ( $10 \mu\text{M}$ ).

#### *Native TRPC5-like currents in the U-87 glioblastoma cell line are blocked by clemizole*

Previous reports confirmed that TRPC5 channels are endogenously expressed in the glioblastoma cell line U-87 (Wang *et al.*, 2009; Richter *et al.*, 2014) and that riluzole-evoked

MOL #93229

calcium signals could be impeded by a siRNA-mediated knock-down of TRPC5 (Richter *et al.*, 2014). Accordingly, riluzole (100  $\mu$ M) provoked currents in whole cell patch clamp recordings on U-87 cells, which could partially be inhibited by clemizole (50  $\mu$ M) (Fig. 5D-F). The riluzole-evoked currents displayed a reversal potential more negative than heterologously expressed TRPC5 channels, together with a stronger inward current (Fig. 5E). As all of the riluzole-evoked inward current disappeared when permeable cations were substituted for NMDG in the extracellular solution (Richter *et al.*, 2014), this would be consistent with the activation of additional potassium channels, which do not respond to clemizole. This could either be caused directly through riluzole or through a TRPC5-mediated increase in  $[Ca^{2+}]_i$ .

## DISCUSSION

In this study we identified clemizole as a novel blocker of TRPC5 channels. Clemizole (1-p-chlorobenzyl-2-(1-pyrrolidinyl) methylbenzimidazole) has originally been developed as a histamine H<sub>1</sub>-receptor antagonist. This first generation antihistamine can pass the blood-brain barrier and has a low toxicity (Wansker, 1962; Einav *et al.*, 2010). It was developed in the 1950`s to treat allergic reactions and various dermatological diseases (Zierz and Greither, 1952; Jacques and Fuchs, 1960). Besides its anti-histaminergic action, clemizole inhibits monoamine reuptake in the brain (Oishi *et al.* 1994) and blocks hERG channels at a concentration of 10  $\mu$ M (data obtained from <http://pubchem.ncbi.nlm.nih.gov>). Nowadays, clemizole is not marketed as a single agent antihistamine anymore. However, clemizole might be beneficial in the treatment of hepatitis C (HCV) infections. It has been shown to inhibit the binding of NS4B to HCV RNA, exhibiting moderate antiviral effects against hepatitis C virus (genotype 2a, EC<sub>50</sub> = 8  $\mu$ M) on its own (Einav *et al.*, 2008). Combining clemizole with HCV protease inhibitors proved to be highly synergistic, strongly enhancing the potency of such therapeutics (Einav *et al.*, 2010). Moreover, a recent study of Baraban *et al.* reported that clemizole inhibits spontaneous seizures in a zebrafish model for Dravet syndrome (scn1Lab mutant), a rare and severe form of monogenic epilepsy, which is mainly caused by mutations in Nav1.1 (SCN1A), a voltage-gated sodium channel (Baraban *et al.*, 2013; Catterall, 2014). However, high concentrations of 100  $\mu$ M clemizole were needed to suppress spontaneous hyperactivity.

We here identified clemizole as a novel blocker of TRPC5 channels. Clemizole potently inhibited TRPC5 channels and exhibited a moderate selectivity within the TRPC family, with a 6-fold selectivity (in calcium assays) over its closest homologue TRPC4 $\beta$ . The inhibition was effective towards different modes of TRPC5 activation, such as stimulation of GPCR, hypotonic buffer conditions or a direct activation by riluzole. We assume that clemizole directly acts on TRPC5 channels as the drug was still effective in excised inside-out patches,

where intracellular components are washed out. As clemizole is a lipophilic compound ( $\log P = 4.23$ ; chemicalize.org), we cannot clearly discriminate between an intracellular or extracellular site of action on TRPC5 channels but the delayed onset of action in the inside-out measurements with a latency of 20 – 30 s might hint to a necessity of clemizole to reach the extracellular site of the channel.

TRPC5 channels can assemble as homo- or heterotetramers with TRPC1 or TRPC4 (Schaefer *et al.*, 2000; Strubing *et al.*, 2003), exhibiting distinct biophysical properties (Strubing *et al.*, 2001). Since TRPC5 and TRPC1 show overlapping expression pattern in mammalian brain tissue (Strubing *et al.*, 2001), we analysed the effect of clemizole on heteromeric TRPC1:TRPC5 complexes. As reported previously, TRPC1:TRPC5 heteromers in HEK293 cells were stimulated by riluzole. The same applies for TRPC5 or possible TRPC1:TRPC5 heteromers, endogenously expressed in the U-87 glioblastoma/astrocytoma cell line (Richter *et al.*, 2014). Such riluzole-induced currents were blocked upon clemizole application, indicating that clemizole also targets heteromeric TRPC5 channels and might be effective in native tissues. Because of its lipophilic properties, clemizole is able to pass the blood-brain barrier. It will be the aim of future studies to test whether application of clemizole or other TRPC5 inhibitors *in vivo* mimics the anxiolytic-like and kidney-protective phenotype of TRPC5-deficient mice (Riccio *et al.*, 2009; Puram *et al.*, 2011; Schaldecker *et al.*, 2013). With regard to future *in vivo* experiments, clemizole has the advantage of having been intensively studied since it was used for its antihistaminic effect. The safety and tolerability of clemizole to treat hepatitis C has been investigated in a clinical trial at a dosage of 200 mg/d (CLEAN-1 trial, NCT00945880) but its outcome has not been reported, yet. According to the current state of knowledge, clemizole might serve as a promising starting point for the development of pharmacological tools, which provide new insights into the physiological relevance of TRPC5 expressed in native systems and which are possibly applicable for the establishment of new therapeutic strategies targeting TRPC5 in diseases.



MOL #93229

### **Acknowledgements**

Stable myc-tagged rat HEK<sub>TRPM3</sub> cell line was a kind gift from S. Philipp (Universität des Saarlandes, Homburg, Germany). We thank Nicole Urban for excellent technical assistance.

### **Authorship Contribution**

Participated in research design: Richter, Schaefer, and Hill

Conducted experiments: Richter and Hill

Contributed new reagents or analytic tools:

Performed data analysis: Richter and Hill

Wrote or contributed to the writing of the manuscript: Richter, Schaefer, and Hill

## References

Baraban M, Anselme I, Schneider-Maunoury S and Giudicelli F (2013) Zebrafish embryonic neurons transport messenger RNA to axons and growth cones in vivo. *J Neurosci* **33**: 15726-15734.

Catterall WA (2014) Sodium channels, inherited epilepsy, and antiepileptic drugs. *Annu Rev Pharmacol Toxicol* **54**: 317-338.

Einav S, Gerber D, Bryson PD, Sklan EH, Elazar M, Maerkl SJ, Glenn JS and Quake SR (2008) Discovery of a hepatitis C target and its pharmacological inhibitors by microfluidic affinity analysis. *Nat Biotechnol* **26**: 1019-1027.

Einav S, Sobol HD, Gehrig E and Glenn JS (2010) The hepatitis C virus (HCV) NS4B RNA binding inhibitor clemizole is highly synergistic with HCV protease inhibitors. *J Infect Dis* **202**: 65-74.

Fowler MA, Sidiropoulou K, Ozkan ED, Phillips CW and Cooper DC (2007) Corticolimbic expression of TRPC4 and TRPC5 channels in the rodent brain. *PLoS One* **2**: e573.

Fruhwald J, Camacho Londono J, Dembla S, Mannebach S, Lis A, Drews A, Wissenbach U, Oberwinkler J and Philipp SE (2012) Alternative splicing of a protein domain indispensable for function of transient receptor potential melastatin 3 (TRPM3) ion channels. *J Biol Chem* **287**: 36663-36672.

Gardam KE, Geiger JE, Hickey CM, Hung AY and Magoski NS (2008) Flufenamic acid affects multiple currents and causes intracellular Ca<sup>2+</sup> release in *Aplysia* bag cell neurons. *J Neurophysiol* **100**: 38-49.

Greka A and Mundel P (2011) Balancing calcium signals through TRPC5 and TRPC6 in podocytes. *J Am Soc Nephrol* **22**: 1969-1980.

Greka A, Navarro B, Oancea E, Duggan A and Clapham DE (2003) TRPC5 is a regulator of hippocampal neurite length and growth cone morphology. *Nat Neurosci* **6**: 837-845.

MOL #93229

Hill K and Schaefer M (2007) TRPA1 is differentially modulated by the amphipathic molecules trinitrophenol and chlorpromazine. *J Biol Chem* **282**: 7145-7153.

Hofmann T, Obukhov AG, Schaefer M, Harteneck C, Gudermann T and Schultz G (1999) Direct activation of human TRPC6 and TRPC3 channels by diacylglycerol. *Nature* **397**: 259-263.

Hofmann T, Schaefer M, Schultz G and Gudermann T (2002) Subunit composition of mammalian transient receptor potential channels in living cells. *Proc Natl Acad Sci U S A* **99**: 7461-7466.

Hu HZ, Gu Q, Wang C, Colton CK, Tang J, Kinoshita-Kawada M, Lee LY, Wood JD and Zhu MX (2004) 2-aminoethoxydiphenyl borate is a common activator of TRPV1, TRPV2, and TRPV3. *J Biol Chem* **279**: 35741-35748.

Hui H, McHugh D, Hannan M, Zeng F, Xu SZ, Khan SU, Levenson R, Beech DJ and Weiss JL (2006) Calcium-sensing mechanism in TRPC5 channels contributing to retardation of neurite outgrowth. *J Physiol* **572**: 165-172.

Inoue R, Okada T, Onoue H, Hara Y, Shimizu S, Naitoh S, Ito Y and Mori Y (2001) The transient receptor potential protein homologue TRP6 is the essential component of vascular alpha(1)-adrenoceptor-activated Ca(2+)-permeable cation channel. *Circ Res* **88**: 325-332.

Jacques AA and Fuchs VH (1960) Clinical evaluation of clemizole in allergic rhinitis. *Int Rec Med* **173**: 88-91.

Kovacs G, Montalbetti N, Simonin A, Danko T, Balazs B, Zsembery A and Hediger MA (2012) Inhibition of the human epithelial calcium channel TRPV6 by 2-aminoethoxydiphenyl borate (2-APB). *Cell Calcium* **52**: 468-480.

Lenz JC, Reusch HP, Albrecht N, Schultz G and Schaefer M (2002) Ca<sup>2+</sup>-controlled competitive diacylglycerol binding of protein kinase C isoenzymes in living cells. *J Cell Biol* **159**: 291-302.

Li M, Jiang J and Yue L (2006) Functional characterization of homo- and heteromeric channel kinases TRPM6 and TRPM7. *J Gen Physiol* **127**: 525-537.

Lievremont JP, Bird GS and Putney JW, Jr. (2005) Mechanism of inhibition of TRPC cation channels by 2-aminoethoxydiphenylborane. *Mol Pharmacol* **68**: 758-762.

Merritt JE, Armstrong WP, Benham CD, Hallam TJ, Jacob R, Jaxa-Chamiec A, Leigh BK, McCarthy SA, Moores KE and Rink TJ (1990) SK&F 96365, a novel inhibitor of receptor-mediated calcium entry. *Biochem J* **271**: 515-522.

Miller M, Shi J, Zhu Y, Kustov M, Tian JB, Stevens A, Wu M, Xu J, Long S, Yang P, Zholos AV, Salovich JM, Weaver CD, Hopkins CR, Lindsley CW, McManus O, Li M and Zhu MX (2011) Identification of ML204, a novel potent antagonist that selectively modulates native TRPC4/C5 ion channels. *J Biol Chem* **286**: 33436-33446.

Miller MR, Shi J, Wu M, Engers J, Hopkins CR, Lindsley CW, Salovich JM, Zhu Y, Tian JB, Zhu MX, McManus OB and Li M (2010) Novel Chemical Inhibitor of TRPC4 Channels. In: *Probe Reports from the NIH Molecular Libraries Program* (Bethesda (MD)).

Norenberg W, Sobottka H, Hempel C, Plotz T, Fischer W, Schmalzing G and Schaefer M (2012) Positive allosteric modulation by ivermectin of human but not murine P2X7 receptors. *Br J Pharmacol* **167**: 48-66.

Oishi R, Shishido S, Yamori M and Saeki K (1994) Comparison of the effects of eleven histamine H<sub>1</sub>-receptor antagonists on monoamine turnover in the mouse brain. *Naunyn Schmiedebergs Arch Pharmacol*. **349**: 140-144.

Puram SV, Riccio A, Koirala S, Ikeuchi Y, Kim AH, Corfas G and Bonni A (2011) A TRPC5-regulated calcium signaling pathway controls dendrite patterning in the mammalian brain. *Genes Dev* **25**: 2659-2673.

Riccio A, Li Y, Moon J, Kim KS, Smith KS, Rudolph U, Gapon S, Yao GL, Tsvetkov E, Rodig SJ, Van't Veer A, Meloni EG, Carlezon WA, Jr., Bolshakov VY and Clapham DE (2009) Essential role for TRPC5 in amygdala function and fear-related behavior. *Cell* **137**: 761-772.

Richter JM, Schaefer M and Hill K (2014) Riluzole activates TRPC5 channels independently of PLC activity. *Br J Pharmacol* **171**: 158-170.

Schaefer M, Albrecht N, Hofmann T, Gudermann T and Schultz G (2001) Diffusion-limited translocation mechanism of protein kinase C isotypes. *FASEB J* **15**: 1634-1636.

Schaefer M, Plant TD, Obukhov AG, Hofmann T, Gudermann T and Schultz G (2000) Receptor-mediated regulation of the nonselective cation channels TRPC4 and TRPC5. *J Biol Chem* **275**: 17517-17526.

Schaldecker T, Kim S, Tarabanis C, Tian D, Hakrrouch S, Castonguay P, Ahn W, Wallentin H, Heid H, Hopkins CR, Lindsley CW, Riccio A, Buvall L, Weins A and Greka A (2013) Inhibition of the TRPC5 ion channel protects the kidney filter. *J Clin Invest* **123**: 5298-5309.

Strubing C, Krapivinsky G, Krapivinsky L and Clapham DE (2001) TRPC1 and TRPC5 form a novel cation channel in mammalian brain. *Neuron* **29**: 645-655.

Strubing C, Krapivinsky G, Krapivinsky L and Clapham DE (2003) Formation of novel TRPC channels by complex subunit interactions in embryonic brain. *J Biol Chem* **278**: 39014-39019.

Urban N, Hill K, Wang L, Kuebler WM and Schaefer M (2012) Novel pharmacological TRPC inhibitors block hypoxia-induced vasoconstriction. *Cell Calcium* **51**: 194-206.

Wang B, Li W, Meng X and Zou F (2009) Hypoxia up-regulates vascular endothelial growth factor in U-87 MG cells: involvement of TRPC1. *Neurosci Lett* **459**: 132-136.

Wansker BA (1962) Clemizole hydrochloride: a clinical evaluation of its antipruritic effect. *Skin (Los Angeles)* **1**: 157-159.

Xu SZ, Zeng F, Boulay G, Grimm C, Harteneck C and Beech DJ (2005) Block of TRPC5 channels by 2-aminoethoxydiphenyl borate: a differential, extracellular and voltage-dependent effect. *Br J Pharmacol* **145**: 405-414.

Zierz P and Greither H (1952) [Clinical evaluation of allercur, a new antihistaminic]. *Arztl Wochensh* **7**: 704-707.

MOL #93229

## Footnotes

This work was supported by the Deutsche Forschungsgemeinschaft [HI 829/2-1]

## Legends for Figures

### Figure 1. Concentration-dependent inhibition of TRPC5 by clemizole

*A-B*, Concentration-response relation of  $\text{Ca}^{2+}$  signals in fluo-4-loaded T-REX<sub>TRPC5</sub> cells (*A*, 48 h Tet+) and parental T-REx cells (*B*). Cells were first treated with different concentrations of clemizole, then a mixture of agonists (300  $\mu\text{M}$  ATP, 300  $\mu\text{M}$  carbachol, 0.5 U/ml thrombin; Amix) was applied. Prior to measurements, T-REX<sub>TRPC5</sub> cells were pre-treated with 2  $\mu\text{M}$  thapsigargin for 5 min to deplete  $\text{InsP}_3$ -sensitive internal  $\text{Ca}^{2+}$  stores. Parental T-REx control cells remained thapsigargin-untreated to determine Amix-induced  $\text{Ca}^{2+}$  release from intracellular stores. The  $\text{IC}_{50}$  value of clemizole was calculated by non-linear curve fitting with the Hill equation. Datapoints display means and SD of 6 (T-REX<sub>TRPC5</sub>) or 8 (parental T-Rex) independent experiments. *C*, Chemical structure of clemizole. *D-F*, Clemizole blocks TRPC5 currents irrespectively of the mode of activation. Representative fura-2-based single cell  $[\text{Ca}^{2+}]_i$  experiments of tetracycline-induced T-REX<sub>TRPC5</sub> cells are shown. Cells were treated with 2  $\mu\text{M}$  thapsigargin, and TRPC5 activity was stimulated with Amix (*D*), 50  $\mu\text{M}$  riluzole (*E*) or hypoosmotic (200 mosmol / kg) HBS buffer (*F*), followed by addition of 10  $\mu\text{M}$  clemizole.

### Figure 2. Electrophysiological characterisation of clemizole-mediated TRPC5 block

Representative patch clamp recordings of whole cell currents in tetracycline-induced T-REX<sub>TRPC5</sub> cells. *A*, Data were extracted from voltage ramps as in *B* and depict current amplitudes at +100 mV (upper trace) and -100 mV (lower trace). *B*, Corresponding *I/V* curves of basal TRPC5 currents (*1*) and upon Amix- (*2*), and clemizole (10  $\mu\text{M}$ )-treatment (*3*) taken at time points indicated in (*A*). *C*, Statistical evaluation of 4 independent experiments such as in *A* (\**P* < 0.05). *D*, TRPC5 currents were repetitively stimulated with 50  $\mu\text{M}$  riluzole.

MOL #93229

Clemizole was added at 10  $\mu\text{M}$ . *E*, Corresponding I/V curves before (1) and after treatment with riluzole (2) and clemizole (3), taken at time points indicated in D. *F*, Statistical analysis of 6 independent experiments such as in D (\*  $P < 0.05$ ). Data represent means and SEM. *G*, Concentration-response curve of Amix-induced T-REX<sub>TRPC5</sub> whole-cell currents at +100 mV (upper curve) and -100 mV (lower curve) treated with different concentrations of clemizole ( $n > 4$  for each individual data point). The basal current is indicated by the dashed line.

**Figure 3.** Clemizole-mediated block of TRPC5 is independent from intracellular components.

*A-C*, Representative whole cell patch clamp recording of currents in a tetracycline-induced T-REX<sub>TRPC5</sub> cell in the presence of GTP $\gamma$ S (500  $\mu\text{M}$ ) in the patch pipette. *A*, Data were taken from voltage ramps such as in B and display current densities at +100 mV (upper trace) and -100 mV (lower trace). *B*, I/V curves directly after break-in into the whole cell configuration (1), upon GTP $\gamma$ S stimulation (2) and 10  $\mu\text{M}$  clemizole treatment (3). *C*, Statistical analysis of 7 independent experiments such as in A (\*  $P < 0.05$ ). *D, E*, Clemizole blocks riluzole-activated TRPC5 currents in excised inside-out patches. *D*, Representative inside-out patch, containing at least two TRPC5 channels recorded at -80 mV. Channel activity was elicited by 100  $\mu\text{M}$  riluzole, followed by application of 20  $\mu\text{M}$  clemizole. Openings and closures of TRPC5 channels from the same recording are depicted below on an expanded time scale. *E*, Statistical analysis for several independent recordings ( $n = 11$ ) as shown in D. The NPo was averaged for 30s intervals directly before and after activation with riluzole, and 30s after treatment with clemizole.

**Figure 4.** Clemizole-mediated effect on other TRP channels.



MOL #93229

*A-D*,  $\text{Ca}^{2+}$  signals of fluo-4-loaded cells, which overexpress other canonical TRP channels. Thapsigargin pre-treated cells were challenged with different concentrations of clemizole (grey circles) and then treated with a channel-specific agonist (black circles): Amix (TRPC3, C6, C7); carbachol (300  $\mu\text{M}$ , TRPC4 $\beta$ ). Each datapoint displays the mean and SD of at least 4 independent experiments ( $*P < 0.05$ ). *D*, HEK293 cells co-transfected with TRPC4 $\beta$  and M3 $\Delta$ i3R-encoding expression plasmids (HEK<sub>TRPC4 $\beta$ -M3 $\Delta$ i3R</sub>). *E-G*, Representative whole cell patch clamp measurement of currents in a HEK<sub>TRPC4 $\beta$ -M3 $\Delta$ i3R</sub> cell. Data were extracted from voltage ramps and depict current densities at +100 mV (upper trace) and -100 mV (lower trace). *F*, I/V curves of basal TRPC4 $\beta$  currents (1) and upon additive treatment with 300  $\mu\text{M}$  carbachol (2), 10  $\mu\text{M}$  clemizole (3) and 75  $\mu\text{M}$  2-APB (4). Time points of the respective ramps are indicated in E. *G*, Statistical analysis of 7 independent experiments such as in E ( $*P < 0.05$ ). Data represent means and SEM. *H*, Concentration-response curve of carbachol-induced TRPC4 $\beta$  whole-cell currents at +100 mV (upper curve) and -100 mV (lower curve) treated with different concentrations of clemizole ( $n > 3$  for each individual data point). The basal current is indicated by the dashed line.

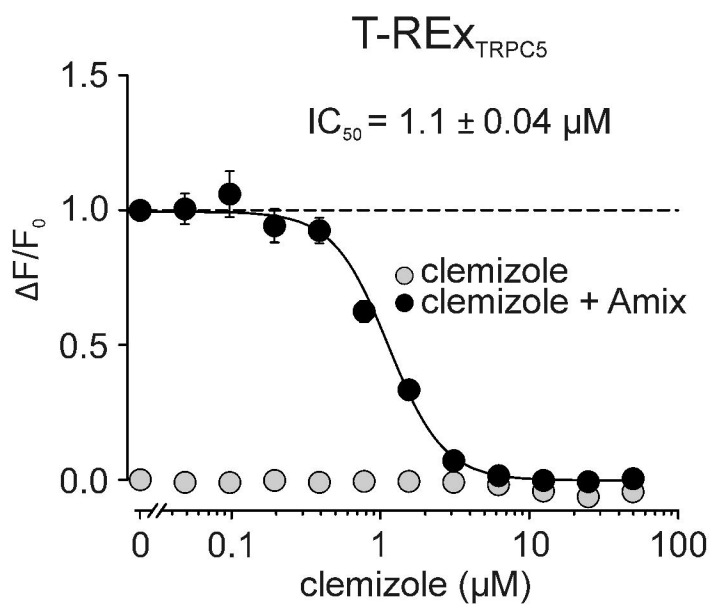
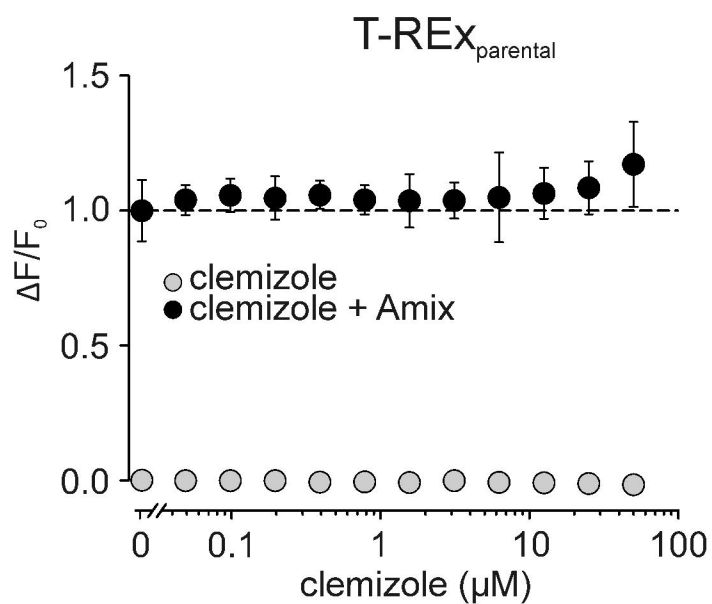
**Figure 5.** Clemizole blocks riluzole-activated heteromeric TRPC1:TRPC5 and endogenously expressed TRPC5 channels in U87 glioblastoma cells

*A-C*, Representative whole cell measurement of HEK293 cells, transiently transfected with TRPC1- and TRPC5-encoding expression plasmids (HEK<sub>TRPC1:TRPC5</sub>). *A*, Data were extracted from voltage ramps and show current densities at +100 mV (upper trace) and -100 mV (lower trace). Cells were treated with 50  $\mu\text{M}$  riluzole and 10  $\mu\text{M}$  clemizole. *B*, I/V curves of basal TRPC1:TRPC5 currents (1) and upon riluzole (2) and clemizole (3) application. *C*, Statistical analysis of 6 independent experiments such as in A ( $*P < 0.05$ ). Data represent means and SEM. *D-F*, Clemizole inhibits TRPC5-like channels endogenously expressed in the U-87

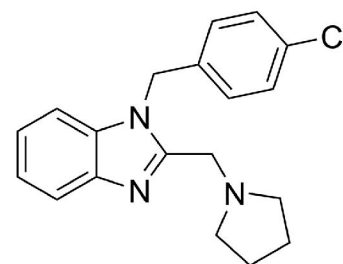
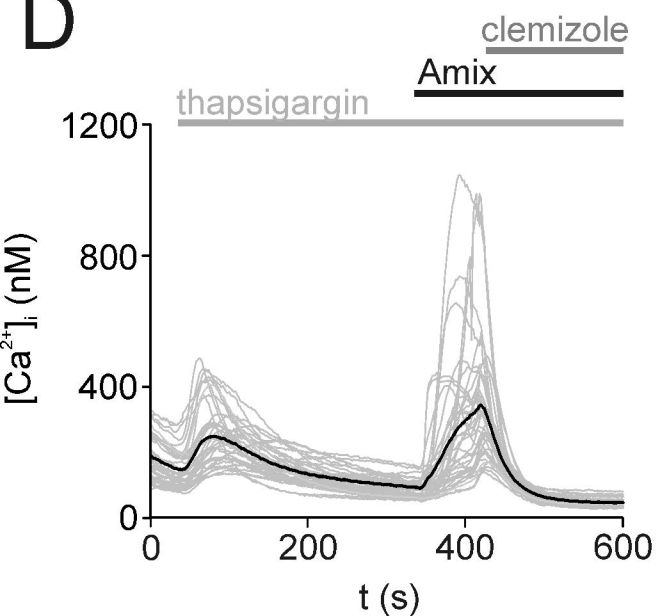
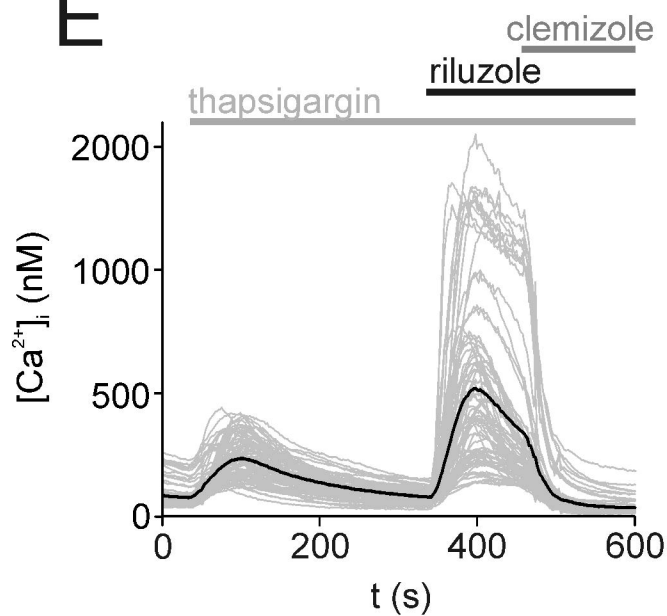
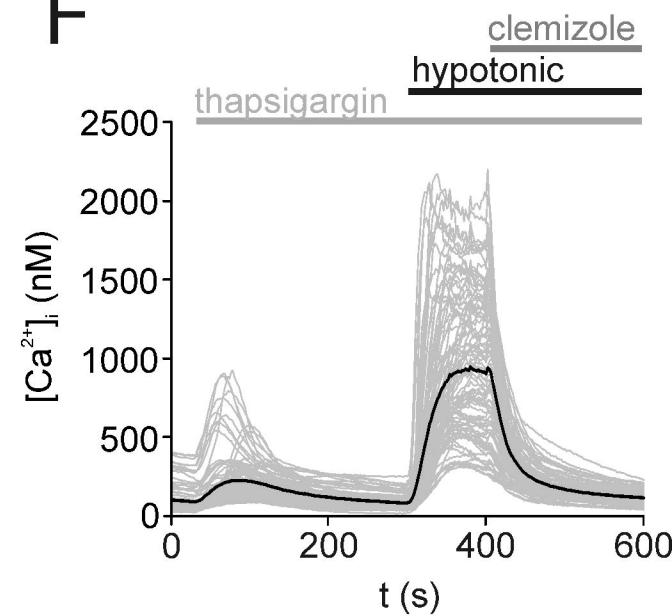
MOL #93229

glioblastoma cell line. Representative whole cell patch clamp recordings of a U-87 cell treated with riluzole (100  $\mu$ M) and clemizole (50  $\mu$ M). *D*, Traces were taken from voltage ramps and depict current densities at +100 mV (upper trace) and -100 mV (lower trace). *E*, I/V curves of basal currents (*1*) and upon riluzole (*2*) and clemizole (*3*) application. Inset depicts clemizole-sensitive component of whole-cell current (*2-3*) *F*, Statistical analysis of 7 independent experiments such as in *D*. Data represent peak current densities and are means and SEM (\* $P < 0.05$ ).

# Figure 1

**A****B****C**

Downloaded from molpharm.aspetjournals.org at ASPET Journals on April 19, 2024

**D****E****F**

# Figure 2

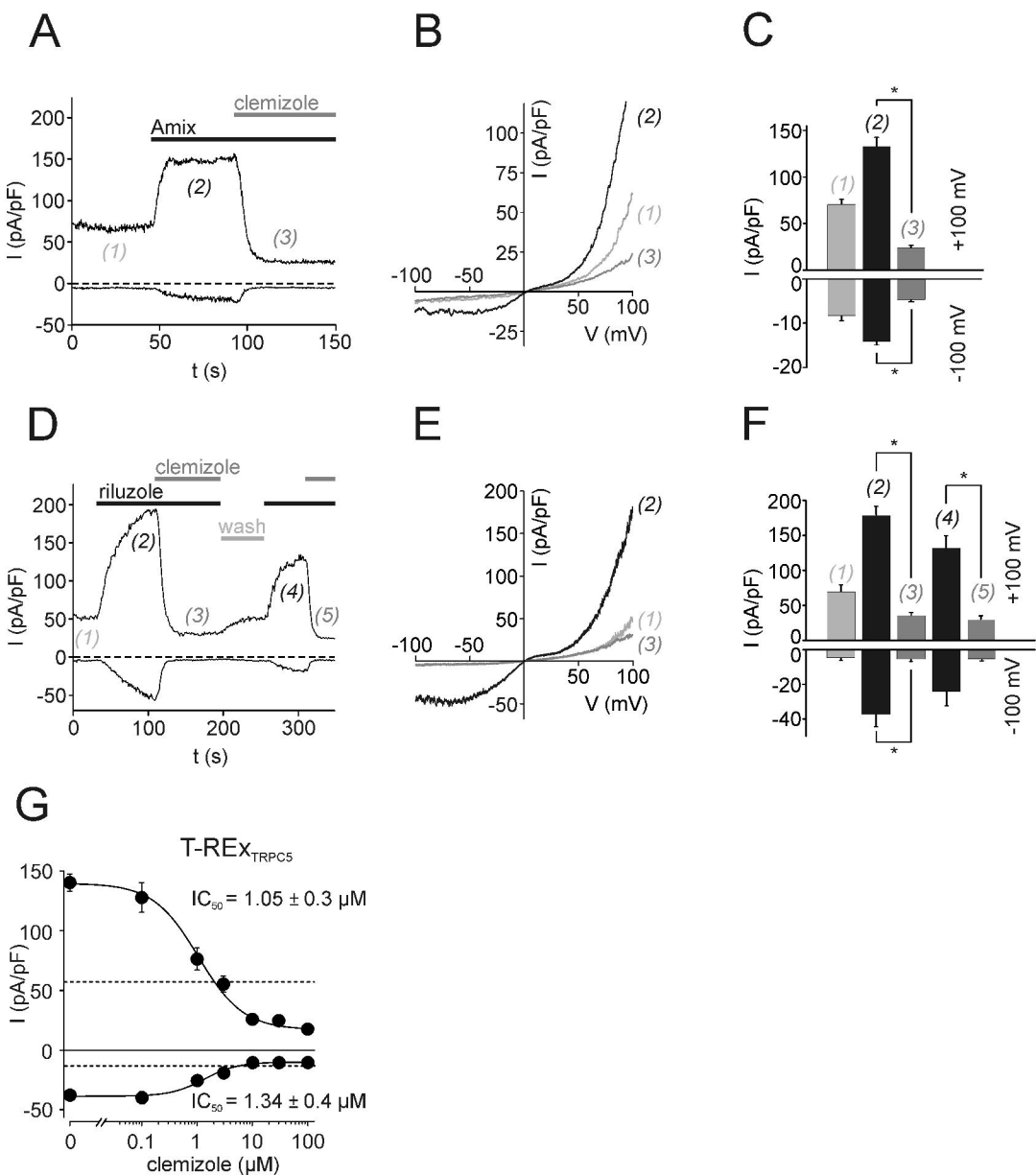


# Figure 3

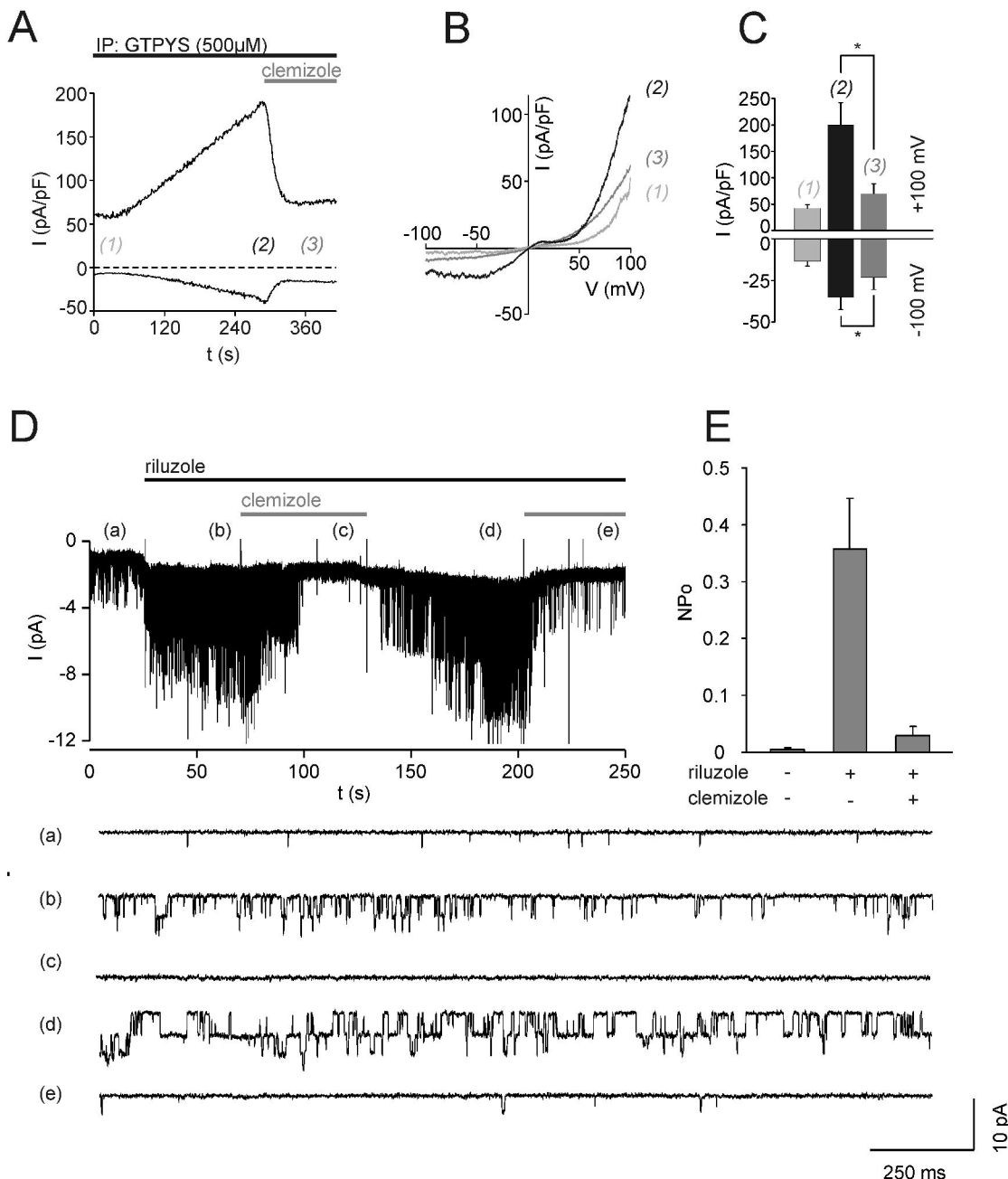


# Figure 4

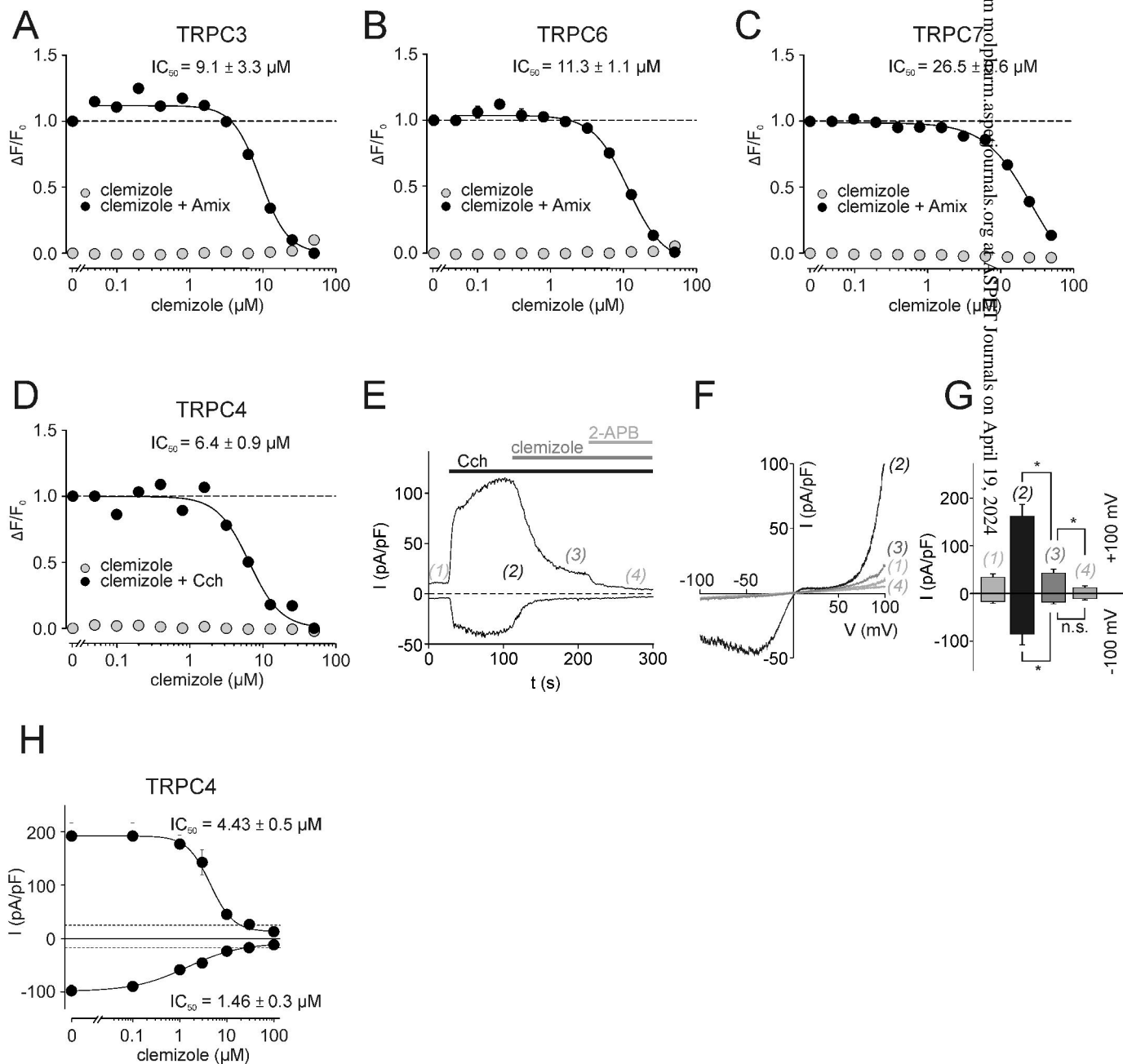


# Figure 5

